INL/RPT-22-69834

Validation of Printed Strain Gauges at Moderate Temperatures (up to 300°C)

October 2022

Advanced Sensors and Instrumentation Program

Timothy L. Phero
Energy and Environmental Science and Technology, Idaho National Laboratory

Michael D. McMurtrey
Nuclear Science and Technology, Idaho National Laboratory

Michael P. Heighes
Nuclear Science and Technology, Idaho National Laboratory

Kaelee A. Novich
Nuclear Science and Technology, Idaho National Laboratory

Idaho National Laboratory

INL is a U.S. Department of Energy National Laboratory
operated by Battelle Energy Alliance, LLC

DISCLAIMER

This information was prepared as an account of work sponsored by an agency of the U.S. Government. Neither the U.S. Government nor any agency thereof, nor any of their employees, makes any warranty, expressed or implied, or assumes any legal liability or responsibility for the accuracy, completeness, or usefulness, of any information, apparatus, product, or process disclosed, or represents that its use would not infringe privately owned rights. References herein to any specific commercial product, process, or service by trade name, trade mark, manufacturer, or otherwise, does not necessarily constitute or imply its endorsement, recommendation, or favoring by the U.S. Government or any agency thereof. The views and opinions of authors expressed herein do not necessarily state or reflect those of the U.S. Government or any agency thereof.

INL/RPT-22-69834
Revision 0

Validation of Printed Strain Gauges at Moderate Temperatures (up to 300°C)

Advanced Sensors and Instrumentation Program

Timothy L. Phero
Energy and Environmental Science and Technology, Idaho National Laboratory
Michael D. McMurtrey
Nuclear Science and Technology, Idaho National Laboratory
Michael P. Heighes
Nuclear Science and Technology, Idaho National Laboratory
Kaelee A. Novich
Nuclear Science and Technology, Idaho National Laboratory

October 2022

Idaho National Laboratory
Idaho Falls, Idaho 83415

http://www.inl.gov

Prepared for the
U.S. Department of Energy
Office of Nuclear Energy
Under DOE Idaho Operations Office
Contract DE-AC07-05ID14517

Page intentionally left blank

ABSTRACT

Strain gauges in material test reactors serve to generate critical mechanical property data for qualifying the performance of reactor components. Resistance-based strain gauge technologies are both well established and commercially available; however, they present limitations in terms of reactor experiment conditions, especially in areas where physical space is a challenge. In this work, an additively manufactured capacitance-based strain gauge was printed on a stainless-steel specimen and tested at up to the prototypic pressurized-water reactor operating temperature of 300°C. In addition, a high-temperature resistive strain gauge (RSG) was used to better understand how the RSGs operate, and to provide baseline measurements for comparison against the printed strain gauges. Future development of printed strain gauges will focus on expanding their temperature limits to 500°C and enabling applications currently beyond the capabilities of commercial RSGs.

Page intentionally left blank

ACKNOWLEDGEMENTS

The authors wish to thank Ashley Lambson for her help in attaching the strain gauges to the test articles. They also thank Thomas Walters and Joel Simpson for their support with the test setup at INL. They thank Kiyo Fujimoto for her help and support regarding the ink materials used for the printed strain gauges. The authors also gratefully acknowledge the support provided by Brian Jaques and David Estrada of Boise State University. This work was supported in part through the Department of Energy (DOE) Advanced Sensors and Instrumentation program under DOE Idaho Operations Office Contract DE-AC07-05ID14517. The views and opinions of authors expressed herein do not necessarily state or reflect those of the U.S. Government or any agency thereof.

Page intentionally left blank

CONTENTS

FIGURES

TABLES

ACRONYMS

AM	Additive manufacturing
BST	Barium strontium titanate
CSG	Capacitive strain gauge
CTE	Coefficient of thermal expansion
IDE	Interdigitated electrode
INL	Idaho National Laboratory
RSG	Resistive strain gauge
RT	Room temperature

Page intentionally left blank

Validation of Printed Strain Gauges at Moderate Temperatures (up to 300°C)

1. INTRODUCTION

Development and continued usage of nuclear energy systems benefit from an increased fundamental understanding of the fuels, cladding types, and structural materials employed in nuclear reactors [1]. Experimentation at irradiation test facilities helps resolve challenges related to these materials; however, due to the harsh conditions generated in such reactors, evaluations of material mechanical properties are often limited to post-irradiation examinations [2]. To expand the capabilities of irradiation test facilities, it is necessary to further understand and develop strain sensing devices that can reliably monitor and provide real-time data on in-core deformation, including expansion/swelling and tensile/creep deformation. Successful deployment of strain sensing devices in reactor conditions requires improved sensor design and manufacturing to enable their application within the wide nuclear test space of current and Gen-IV reactors (i.e., in terms of environment conditions, sample geometry, and materials compatibility) [3]. An increased understanding of currently available strain gauges and the application of direct-write additive manufacturing (AM) approaches can address critical technology gaps in nuclear-relevant strain sensing methodologies.

Resistive strain gauges (RSGs) represent a well-established technology traditionally used to measure localized deformation at strategic locations on a component. Their application for strain measurement extends to a wide variety of high-temperature applications, including nuclear reactors [4]. However, RSGs are confined to wired interconnections and require non-trivial attachment strategies (e.g., welding or epoxy) that can not only affect the underlying component, but also lead to variable sensing performance [2]. Thanks to their relatively low procurement and usage costs, AM technologies may prove able to mitigate the challenges introduced by traditional RSGs (e.g., size limitations and wired interconnections). This enables the exploration and fabrication of specialized devices (i.e., nuclear sensors) that conventional manufacturing by commercial vendors had rendered economically non-viable [5]. Over the last couple of years, AM has demonstrated the capability to fabricate and test in-pile sensors for monitoring peak temperatures [6] and mechanical strain [2]. The material testing enhancements unlocked by these new capabilities help validate modeling and simulation efforts supporting the development, testing, and qualification of new nuclear materials.

In this work, commercial high-temperature RSGs and AM-fabricated capacitive strain gauges (CSGs) were exposed to separate-effects testing (i.e., mechanical strain, temperature) to better understand and qualify their performance at elevated temperatures of up to 300°C. The weldable RSGs were used as a baseline technology for developing the AM-printed CSGs, initially described by Phero et al. [2]. With further development, CSGs could be made compatible with temperatures exceeding 300°C, feature smaller geometries, and operate in various orientations on complex geometries. AM-printed CSGs could potentially support nuclear programs for which size constraints render current RSG technologies inapplicable. Strain gauges could also potentially be used as reference measurements for structural health monitoring in advanced reactors.

2. EXPERIMENTAL METHODS AND MATERIALS

2.1 Strain Gauge Attachment and Fabrication

2.1.1 Weldable Resistive Strain Gauge

Commercially available weldable RSGs (Kyowa) were attached to stainless steel 316 (SS316) tensile specimens fabricated to conform to ASTM E21-09 [7] standards. In this work, two weldable RSG types (i.e., Strain Gauge-A and Strain Gauge-B, seen in Figure 1 and Figure 2) were selected for a strain sensing performance comparison. Both RSGs can measure strain at up to 500°C and are composed of two resistive elements that consist of: a primary active strain sensing element and a secondary dummy element that reduces the temperature effects and allows for active temperature compensation [4]. However, the two RSGs do have a few geometric and material differences that are described in Table 1. Strain gauge geometry and materials are crucial design factors for in-pile experiments featuring limitations in terms of space and/or allowable materials.

Prior to welding the RSG onto the SS316 tensile specimen, the surface was hand-polished with 300-grit paper to remove the oxide layer and any surface impurities. The surface was then cleaned with isopropanol for degreasing. A capacitive discharge single-pulse resistive spot welder was used (Sunstone, CD100SPM) for the welding. The CD100SPM enables micro spot resistance welding, which locally heats the bonding region quickly by discharging a large amount of energy within a span of milliseconds. The spot welder was outfitted with a ≈1 mm handheld probe tip, and the welding was performed at an energy of 30 J, with each tack spaced out at 1/32 in. (0.8 mm). Three strain relief foils were welded onto the test article to secure both the mineral-insulated cabling and the connection block (Figure 1 and Figure 2) prior to welding on the flange containing the sensing region of the RSG. Figure 2 shows the results of welding the RSG strain relief foils and sensing element onto the test article.

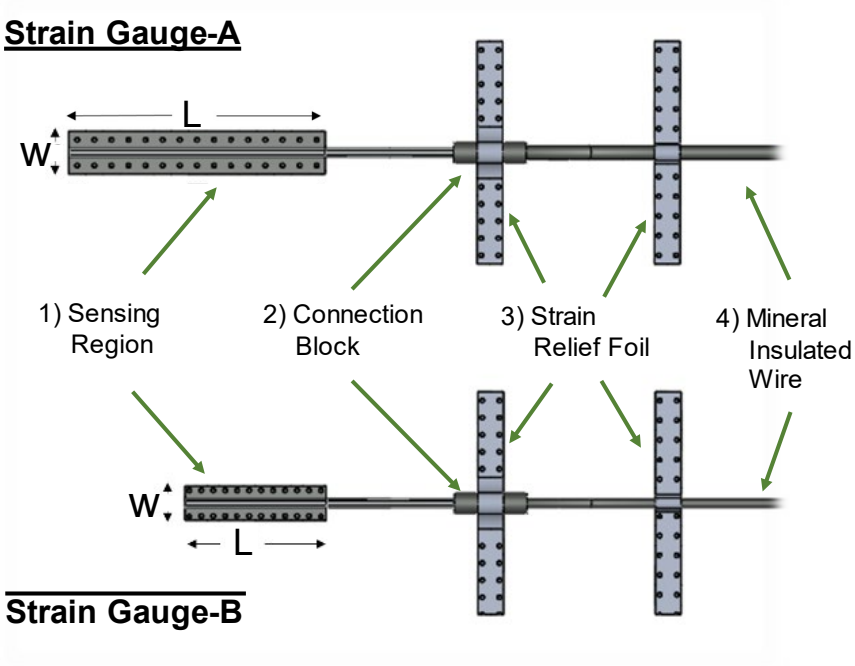

Figure 1. Schematic of the two weldable strain gauge types used in this study (i.e., Strain Gauge-A and Strain Gauge-B). The dimensions and characteristics of the two strain gauges are described in Table 1.

Figure 2. a) Strain Gauge-A and b) Strain Gauge-B, welded onto a SS316 tensile specimen.

Table 1. Relevant dimensions and characteristics of the resistive strain gauges.

	Strain Gauge-A	Strain Gauge-B
Width; W (mm)	5	4
Length; L (mm)	30	16.5
Gauge Length (mm)	20	10
Gauge Resistance (Ω)	120	120
Maximum Operating Temperature (°C)	500–550°C	500–550°C
Adoptable Coefficient of Thermal Expansion ([μm/m]/°C)	12.6	11.7
Material of the Resistive Element	Ni-Cr alloy wire	Ni-Cr alloy wire
Material of the Flange and Tube	SUS321	NCF600
Gauge Type	2-element (half-bridge)	2-element (half-bridge)

The weldable strain gauges were measured using a Wheatstone bridge circuit in a half-bridge configuration. A NI-PXIe-4330 strain bridge module was integrated into a NI-PXIe 1071 chassis and a LabVIEW program that was used for data acquisition. Prior to measurement, an offset and shunt calibration was performed on the strain gauge to correct for any resistance errors stemming from the lead wires and individual resistors within the bridge. A bridge excitation of 2.5 V was used, as this was found to enable stable readings at up to the maximum (i.e., 500–550°C) operating temperature of the strain gauge. The strain gauge's voltage output from the bridge module was converted into strain (ε) via:

$$strain\ (\varepsilon) = \frac{-4 \cdot V_r}{GF \cdot (1+2 \cdot V_r)}, \quad (1)$$

where V_r is the voltage output in V/V and GF is the gauge factor of the strain gauge. The gauge factor is provided by the manufacturer and has a nonlinear relationship with temperature (Figure 3).

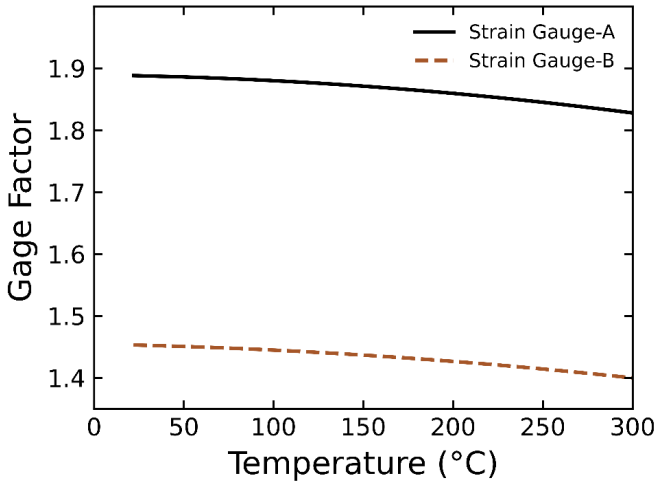

Figure 3. Manufacturer (Kyowa)-provided gauge factors for both types of weldable resistive strain gauge.

2.1.2 Printed Capacitive Strain Gauge

The printed interdigitated electrode (IDE) CSGs (Figure 4) were fabricated using the same methods described in Phero et. al. [2], but were printed onto SS316 instead of aluminum 6061 (Al6061) tensile specimens. This was done to determine whether the IDE CSGs continued to follow the theoretical trends of the discussed analytical models [8,9] and remained efficacious at temperatures up to 300°C on metallic substrates other than Al6061. In their current state, IDE CSGs on SS316 are limited by the use of polyimide insulation/encapsulation. To enable application of printed CSGs in temperatures exceeding 300°C, barium strontium titanate (BST) is being investigated as a feasible ceramic insulation and encapsulation material.

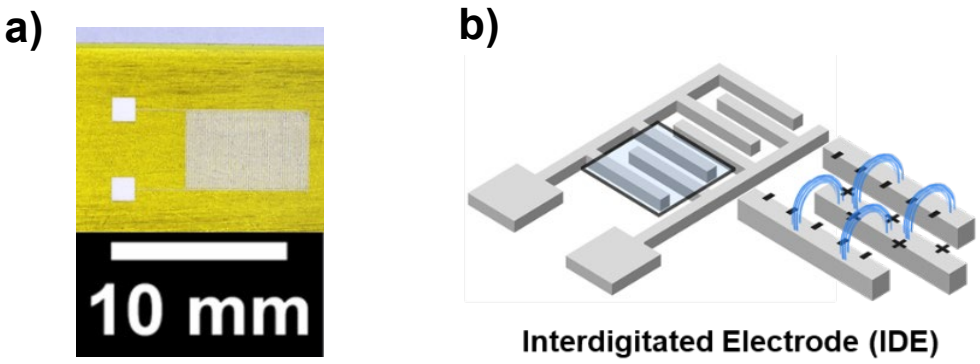

Figure 4. a) Representative image of a strain gauge printed on polyimide insulation that was adhered to a tensile specimen. b) Schematic of the interdigitated electrode design used for the printed capacitive strain gauge.

BST is a printable material [10] observed to experience a change in dielectric constant with mechanical strain [11], making it applicable for strain sensing in harsh environments. 50 nm BST nanopowder were purchased from U.S. Research Nanomaterials, Inc. for formulating a paste material that could be printed using the Voltera V-One printer at Idaho National Laboratory (INL). This formulation involved grinding the nanomaterial with a mortar and pestle, then mixing in ethylene glycol until a paste-like consistency was achieved. Initial formulations of the paste were made at 90 wt% particle loading. The paste was mixed in a centrifugal mixer (Thinky Corporation; ARE-310) at 1500 rpm for 30 seconds, and then at 2200 rpm for 30 seconds. This process was repeated for three cycles until a uniform consistency was achieved. Table 2 shows the Voltera V-One printing parameters utilized to print the BST paste referenced in this work. A thin layer of the paste was also deposited via a rudimentary screen-printing technique that entailed using a 25-µm-thick polyimide tape as a temporary square dam/stencil, then employing a flat edge to scrape a uniform layer of BST material across the surface. The film thickness and surface topography were measured by a 3-D laser scanning confocal microscope (VK-X250, Keyence). The samples were also imaged using an optical microscope (VHX-5000, Keyence).

Table 2. Voltera V-One printer parameters, with the other parameters being set to their default values.

Print Parameter	Value (units)
Nozzle size	225 (µm)
Probe pitch	2 (mm)
Pass spacing	150 (µm)
Standoff distance	100 (µm)
Feed rate	200 (mm/min)
Trim length	50 (mm)
Trim penetration	150 (µm)
Anti-stringing distance	100 (µm)
Kick	350 (µm)
Rheological setpoint	0.50 (unitless)

2.2 High-temperature Test Setup

2.2.1 Mechanical Testing Setup

Each strain gauge was tested up to 1,000 µε for 10 tensile cycles at temperatures ranging from room temperature (RT) to 300°C in order to determine its sensitivity to mechanical strain. More specifically, the CSGs in this work were tested at Boise State University, in the mechanical test fixture described by Phero et al. [2]. The CSG was also tested for its ability to measure compressive strain up to -1000 µε. The performance of the CSG was also tested to determine the effects of being exposed to five thermal cycles up to 300 °C.

The setup for the RSGs was similar, though these were tested at INL. Figure 5 shows the RSG test setup, consisting of a three-zone furnace, a high-temperature extensometer, and two type-K thermocouples (one welded above and one below the strain gauge) to ensure uniform temperature across the gauge region of the tensile specimen. The high-temperature ceramic extensometer was calibrated prior to testing. A preload of 150 N was applied to the sample before being pulled into multiple tensile cycles at a rate of 1.27 mm/min. The test specimens were soaked at the testing temperature for at least an hour to allow the temperatures over the gauge length of tensile specimen to stabilize and remain within ±5°C of each other.

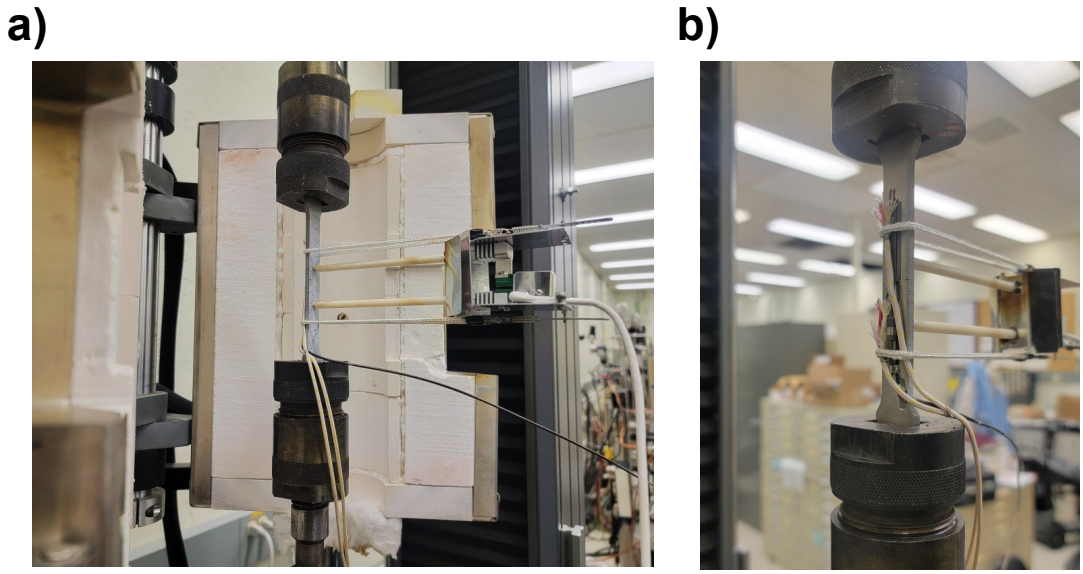

Figure 5. Mechanical test frame setup for testing the commercial resistive strain gauges. a) Furnace and high-temperature extensometer. b) Specimen with the strain gauge and type-K thermocouples welded on.

2.2.2 Temperature Testing Setup

To test the thermal response of the RSGs, Strain Gauge-A and Strain Gauge-B were welded onto SS316 substrates and exposed to temperatures of up to 300°C in air. The specimen was allowed to thermally expand without any external mechanical load (i.e., the top grips were not attached) constraining its inherent expansion during heating. The thermocouple and RSG output were simultaneously recorded in LabVIEW. An unattached (i.e., not welded onto a substrate) Strain Gauge-A was also heated to 300°C for comparison against the Strain Gauge-A bound to the substrate.

3. RESULTS AND DISCUSSION

3.1 Testing of Commercial Weldable Resistive Strain Gauges

3.1.1 Mechanical Testing

Figure 6 shows the strain responses of Strain Gauge-A and the calibrated extensometer at temperatures ranging from RT up to 300°C. The plots show five tensile cycles that are representative of the mechanical testing performed at each temperature. For Strain Gauge-A, the RSG output very closely matched the strain output from the extensometer at all four temperatures. On the other hand, Figure 7 shows that Strain Gauge-B underestimated the actual strain collected from the extensometer at all four temperatures. The plateau in the lower strain measurements at RT (shown in Figure 7a) is caused by the slack in the grips used in the mechanical test fixture, due to an insufficient pre-load on the specimen prior to testing. The results from Strain Gauge-A and Strain Gauge-B are compiled in Figure 8 for direct comparison with the calibrated extensometer. Strain Gauge-A closely matches the extensometer at all four temperatures and at up to the maximum strain of 1000 με; however, Strain Gauge-B begins to deviate from the ideal trend at strains beyond 100–200 με. This difference may be attributable to the different materials used for the strain gauges (see Table 1). The flange material of Strain Gauge-A is an austenitic stainless steel (i.e., SUS321) with an elastic modulus (195 GPa at RT) similar to that of the SS316 tensile specimen. The flange material of Strain Gauge-B, however, is a nickel-based alloy (i.e., NCF600; Table 1) with a slightly higher elastic modulus (215 GPa at RT). This mismatch in elastic moduli carries implications affecting the stresses observed on the sensor under an applied mechanical load.

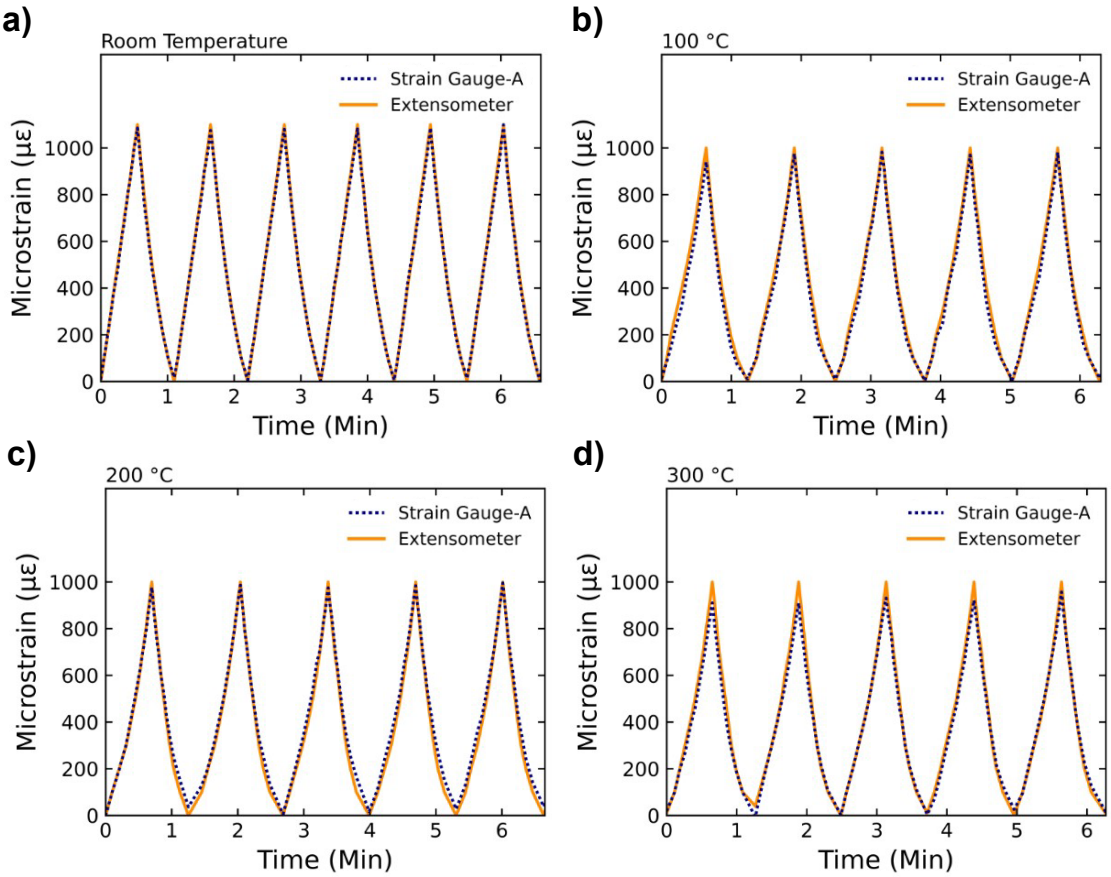

Figure 6. Strain output for Strain Gauge-A while pulling the specimen in tension at environmental temperatures of a) RT, b) 100°C, c) 200°C, and d) 300°C.

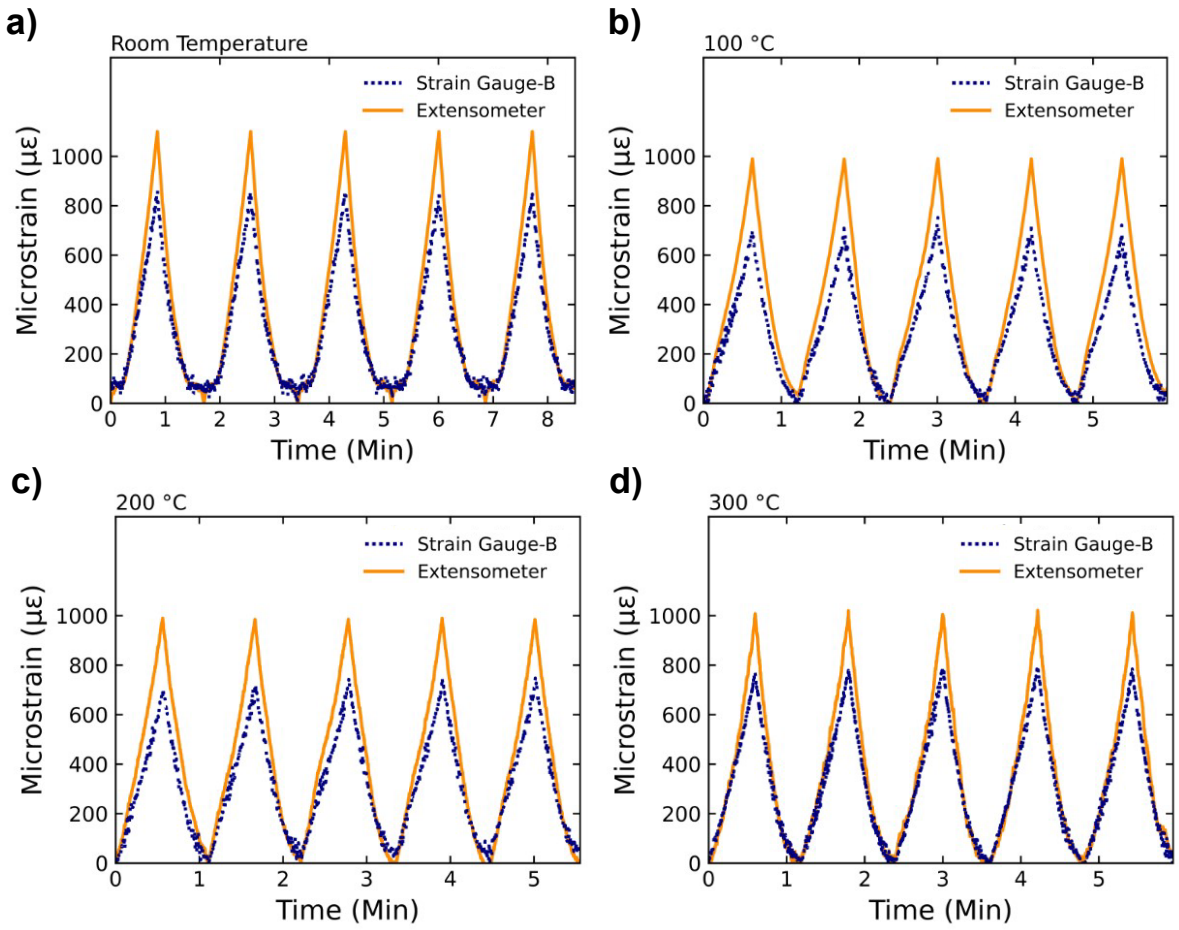

Figure 7. Strain output for Strain Gauge-B while pulling the specimen in tension under environmental temperatures of a) RT, b) 100°C, c) 200°C, and d) 300°C.

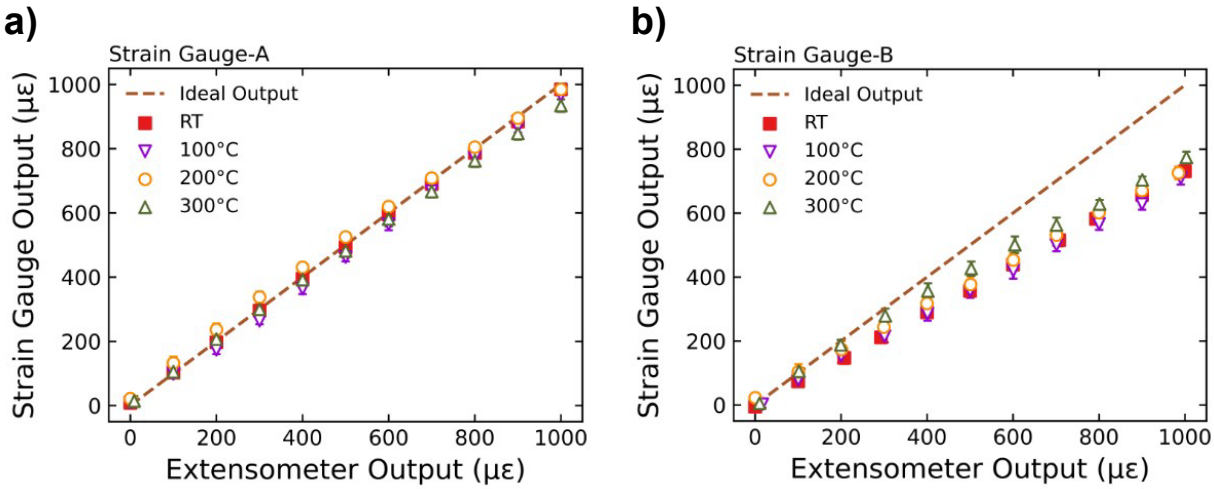

Figure 8. The results from the a) Strain Gauge-A and b) Strain Gauge-B that were welded onto SS316 tensile specimens, in comparison with the strain output from a calibrated high-temperature extensometer.

3.1.2 Temperature Testing – Thermal Strain

Figure 9 shows the thermal responses from the Strain Gauge-A and Strain Gauge-B that were attached to SS316 specimens while being heated up with no externally applied mechanical strain. Strain Gauge-B registered a thermal strain at a rate of 47.4 με/°C, whereas Strain Gauge-A registered a thermal strain at a rate of 38.5 με/°C—a 22.9% difference between the readings of the two strain gauges. These RSGs are self-temperature-compensation gauges, meaning that the elements are heat-treated to offset the difference between the coefficients of thermal expansion (CTEs) of the strain gauge and the specimen to which it is welded. To correctly read the thermal strain on a specimen, it is important to choose an RSG that was heat-treated so as to produce an adoptable CTE (Table 1) similar to that of the substrate being tested. Both Strain Gauge-A and Strain Gauge-B overestimated the thermal strain of the SS316 specimen, as their adoptable CTEs were 12.6 and 11.7, respectively. The expected thermal strain of SS316 was calculated based on the mean SS316 CTE of 15.44 (μm/m)/°C [12]. Figure 10 shows the thermal response of the Strain Gauge-A that was not attached to any substrate (i.e., serving as an as-received sensor) and the Strain Gauge-A that was attached to a SS316 substrate. The unattached RSG shows a much higher thermal strain output than the RSG attached to the substrate. This further illustrates the substrate limitations of each RSG, all of which were purposely heat-treated so as to only work on materials with a specific CTE.

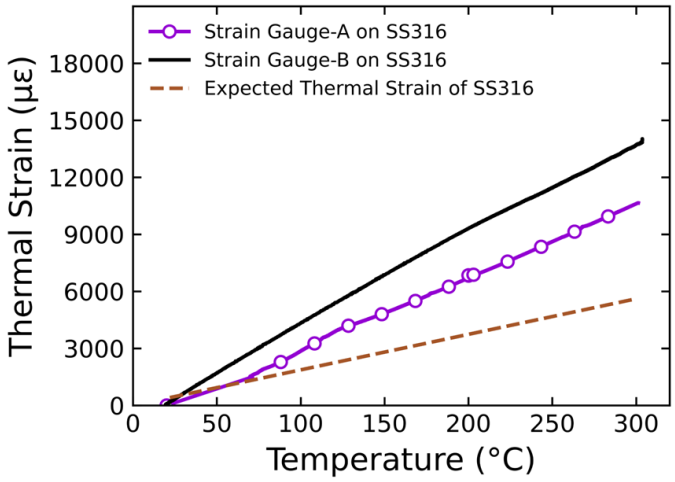

Figure 9. Thermal strain output from the Strain Gauge-A and Strain Gauge-B that were attached to SS316 substrate and heated to 300°C. The expected thermal strain was calculated based on the SS316 CTE.

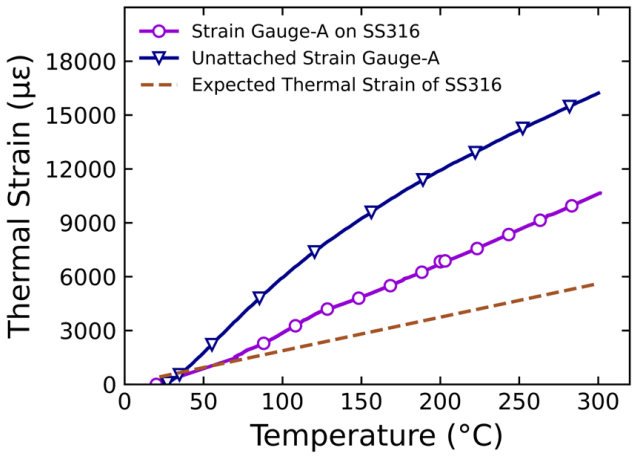

Figure 10. Thermal strain output from the Strain Gauge-A that was unattached and the Strain Gauge-A that was welded to a SS316 substrate. The expected thermal strain was calculated based on the SS316 CTE [12].

3.2 Testing of the Printed Capacitive Strain Gauge

3.2.1 Mechanical Testing

Figure 11 shows the mechanical testing results for the CSG printed on a SS316 tensile specimen. When printed onto a SS316 tensile specimen, the IDE CSG continues to follow the analytical model proposed by Kim et al. [8], and deviates from the model proposed by Hu et al. [9]. In addition, the sensitivity of the strain gauge (i.e., gauge factor) remains relative consistent at 1.01 $(\Delta C/C_0)/(\mu\varepsilon)$ under all four temperatures tested. Furthermore, on SS316, the strain gauge was able to test up to 1000 με at the higher 200 and 300°C temperatures, unlike the trends observed for Al6061 by Phero et al. [2]. This further suggests that the deviations from the Al6061 trends reflect a drastic decrease in the mechanical properties of the substrate, and not a problem with the IDE CSG system itself.

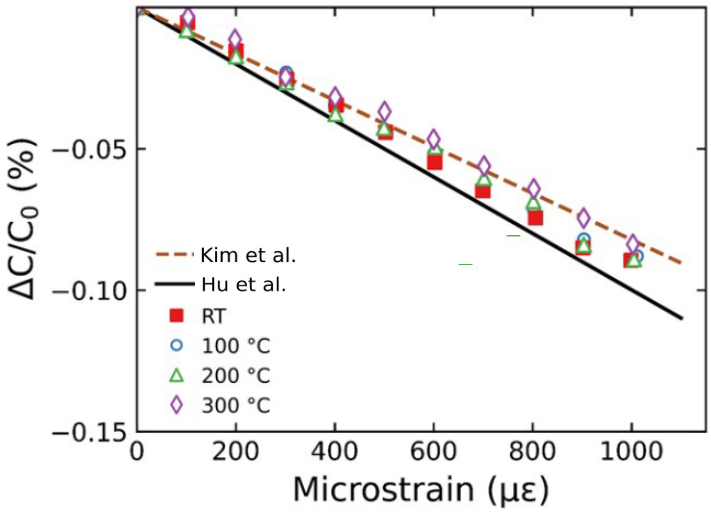

Figure 11. Tensile strain output of a capacitive strain gauge printed onto a SS316 substrate tested at temperatures ranging from RT to 300°C. Despite the substrate change, the output closely matches the results from the analytical models [8,9] previously discussed in Phero et al. [2].

3.2.2 Compression Testing

The CSG response had previously only been tested under tensile strain, since it is the primary strain type expected to be observed on fuel pins under light-water reactor conditions. In other applications, however, compressive strain can also be expected, depending on the experimental environment, the substrate geometry, and the strain gauge's attachment location. To fully qualify the CSG performance, its response to compression was measured through 10 cycles from 0 to -1000 με (Figure 12). As seen in Figure 12, the CSG compression response continued to closely match the theoretical models. A gauge factor of 0.95 was calculated in both the tensile and compressive regions of the test; however, the compression measurement carries a higher degree of uncertainty than the tension measurements. These two tests were performed at different times, making it difficult to distinguish whether this uncertainty stems from the sensor response to compression, or from drifting and measurement uncertainty of the LCR meter [13].

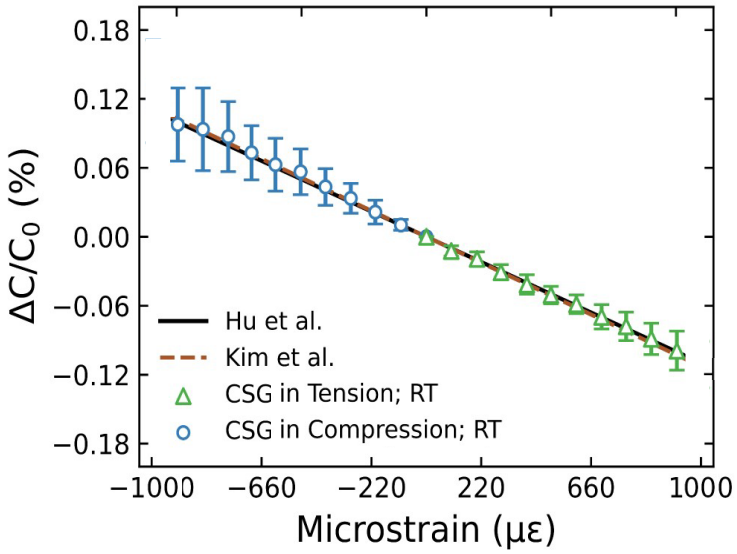

Figure 12. Performance of the CSG that was attached to a SS316 substrate, in terms of the CSG's response to both compression and tensile strain [8,9].

3.2.3 Thermal Cycling Test

To test the reliability of the printed CSG, the strain sensitivity was measured after a thermal cycle that heated the CSG from 22 to 300°C, then cooled it back down to 22°C. After the full thermal cycle, the CSG was tested, in tension, for 10 strain cycles at 22°C. This process was repeated for a total of five thermal cycles. As seen in Figure 13, the gauge factor decreased from 1.01 to 0.86 after the first cycle, then increased and stabilized at 1.16 for cycles 3–5. As mentioned in Phero et al. [2], it is difficult to distinguish whether this change in gauge factor is an effect of thermal cycling or merely the result of drift in the LCR meter used to measure the CSG. The capacitance of the strain gauge was observed to drop from 10.1 to 9.2 pF after the fifth thermal cycle. This is attributed to thermal fatigue having caused the cracking of some electrodes in the IDE structure. The ensuing reduction in neighboring electrode pairs lowers the capacitance of the CSG.

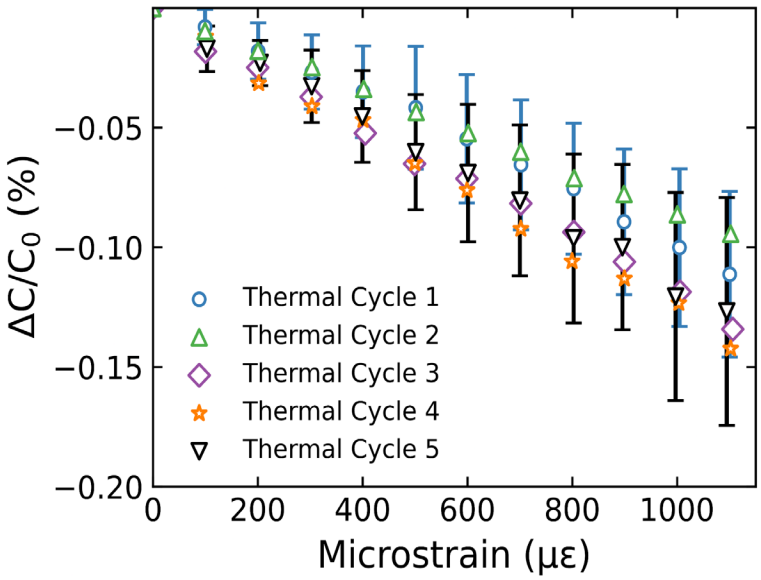

Figure 13. Thermal cycle tests at up to 300°C for multiple cycles; CSG performance tested at RT. The measurement uncertainty for cycles 1 and 5 are shown.

3.3 Formulation of Piezoelectric Material

While the CSG has been successfully tested up to 300°C, material changes will be needed to move its application to higher temperatures. This was supported by on-going efforts to formulate BST paste materials that can be used on the Voltera V-one printer. It was found that BST paste with 90 wt% particle loading deposited relatively consistent and did not clog the printer's nozzle. Figure 14d shows a representative image of a printed BST pad. User laser profilometry, a film thickness of 135 µm was measured. As with the CTE mismatch between the BST and the SS316 substrate, this level of film thickness causes cracking in the film (Figure 15a). The cracking can be mitigated by reducing the film thickness. Figure 15b shows BST applied via a screen-printing technique, with no visible cracking on the surface. The screen-printed BST film had a measured thickness of approximately 55 µm. Since the defects in the BST film carry implications for reducing the dielectric properties, it is advantageous to incorporate manufacturing techniques that would allow for the deposition of thin films. This would mitigate CTE-mismatch-generated cracking when curing the film on SS316 and reduce the potential for delamination or cracking during mechanical testing.

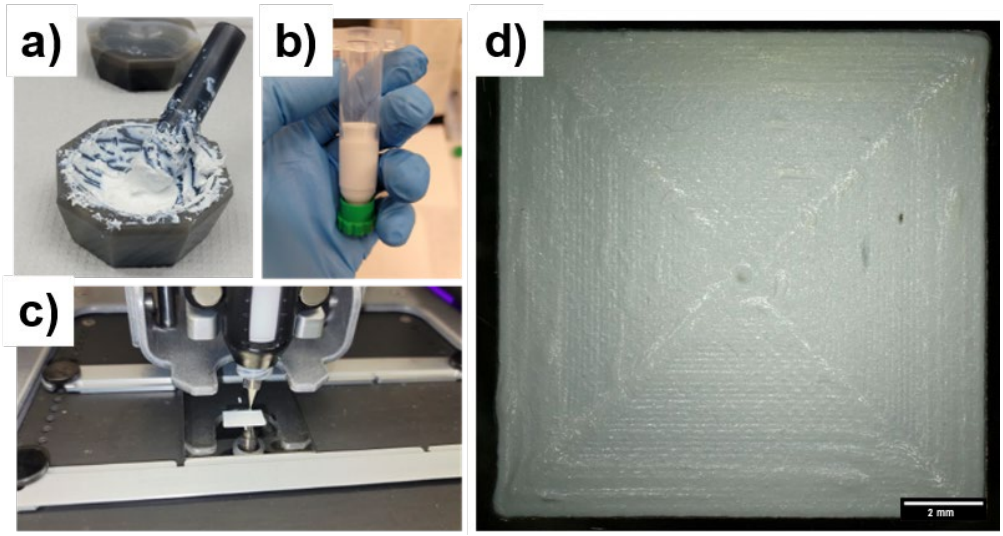

Figure 14. Sequential photos showing the formulation of the ink into a printable pad. a) BST nanoparticles were ground up and mixed with ethylene glycol to enable 90 wt% particle loading. b) The mixed material was loaded into a printer ink cartridge. c) The mixed material was then used to print on the Voltera V-One printer. d) Representaive photo of a printed pad.

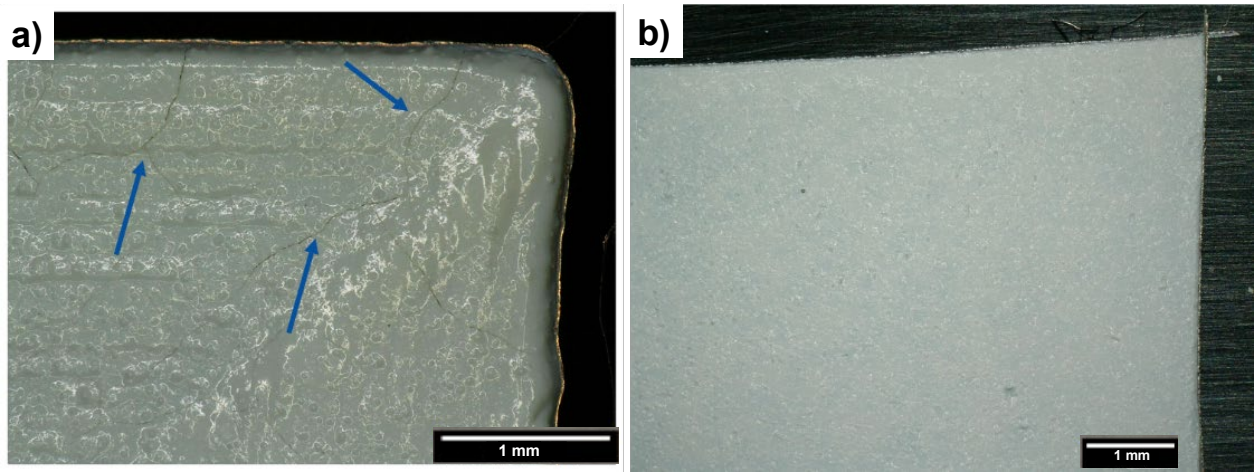

Figure 15. a) A 135-µm-thick BST film printed out by the Voltera V-One printer, revealing cracking caused by excessive film thickness and thermal expansion mismatch. b) A 55-µm-thick BST film that was screen printed with no visible cracking.

4. SUMMARY AND CONCLUSION

By leveraging lessons learned from other industries, AM could potentially be used to develop and deploy strain gauges during both in- and out-of-pile experiments that are not yet possible using commercial technologies. With further development, additive manufactured CSGs could serve to alleviate challenges arising from size constraints, material restrictions, and invasive integration strategies. In their current state, printed CSGs are not ready for nuclear applications; however, this work demonstrates that AM is a viable manufacturing strategy for fabricating functional strain gauges for measuring mechanical strain in environmental temperatures of up to 300°C. Efforts are currently underway to explore the fabrication of IDE CSGs made solely of metal and ceramic constituent layers less susceptible to damage and degradation. This is supported by INL's current capability to develop and optimize additive manufactured ink materials that are application-specific for the printed device. Future development will focus on building upon these initial results by incorporating more robust materials and integration methods, thus extending potential applications of AM CSG to higher temperatures (i.e., up to 500°C).

5. REFERENCES

1. Zinkle, S. J., and G. Was. 2013. "Materials challenges in nuclear energy." *Acta Materialia* 61(3):735-758. https://doi.org/10.1016/j.actamat.2012.11.004.
2. Phero, T. L., et al. 2022. "Additively manufactured strain sensors for in-pile applications." *Sensors and Actuators A: Physical* 344:113691. https://doi.org/10.1016/j.sna.2022.113691.
3. Allen, T., et al. 2008. "Materials challenges for generation IV nuclear energy systems." *Nuclear Technology* 162(3):342-357. https://doi.org/10.13182/NT08-A3961.
4. Pettigrew, M. J. 2013. "The behaviour of weldable strain gauges under nuclear reactor core conditions." *Nuclear Engineering and Design* 263:350-361. https://doi.org/10.1016/j.nucengdes.2013.06.008.
5. Engstrom, D. S., et al. 2014. "Additive nanomanufacturing–A review." *Journal of Materials Research* 29(17):1792-1816. https://doi.org/10.1557/jmr.2014.159.
6. Fujimoto, K. T., et al. 2021. "Additive Manufacturing of Miniaturized Peak Temperature Monitors for In-Pile Applications." *Sensors* 21(22):7688. https://doi.org/10.3390/s21227688.
7. ASTM International. 2014. "Standard Test Methods for Performance Characteristics of Metallic Bonded Resistance Strain Gages." E251-92(2014) 433-452.
8. Kim, S-R., J-H. Kim, and J-W. Park. 2017. "Wearable and Transparent Capacitive Strain Sensor with High Sensitivity Based on Patterned Ag Nanowire Networks." *ACS Applied Materials & Interfaces* 9(31):26407-26416. https://doi.org/10.1021/acsami.7b06474.
9. Hu, C-F., et al. 2013. "Development of 3D carbon nanotube interdigitated finger electrodes on polymer substrate for flexible capacitive sensor application." *Nanotechnology* 24(44):444006. https://iopscience.iop.org/article/10.1088/0957-4484/24/44/444006.
10. Ranasingha, O. K., et al. 2021. "Formulation and Characterization of Sinterless Barium Strontium Titanate (BST) Dielectric Nanoparticle Ink for Printed RF and Microwave Applications." *Journal of Electronic Materials* 50(6):3241-3248. https://doi.org/10.1007/s11664-021-08915-7.
11. Ren, S., et al. 2015. "Investigation of strain gauges based on interdigitated $Ba_{0.5}Sr_{0.5}TiO_3$ thin film capacitors." *Sensors and Actuators A: Physical* 236:159-163. https://doi.org/10.1016/j.sna.2015.11.001.
12. Desai, P. D., and C. Y. Ho. 1978. "Thermal linear expansion of nine selected AISI stainless steels." Thermophysical and Electronic Properties Information Analysis Center, Lafayette, IN. https://apps.dtic.mil/sti/citations/ADA129159.

13. Keysight Technologies. 2014. “Migrating from a Keysight 4284A LCR Meter to a Keysight E4980A Precision LCR Meter - Technical Overview. https://www.keysight.com/us/en/assets/7018-08612/technical-overviews/5989-4434.pdf.